

Hydrogen hopping rates and hydrogen-hydrogen interactions in PdH_x

L. A. Nygren* and R. G. Leisure

Department of Physics, Colorado State University, Fort Collins, Colorado 80523

(Received 1 August 1988; revised manuscript received 31 October 1988)

Ultrasonic-attenuation measurements have been performed on single-crystal PdH_x over the temperature range 80–300 K and for 0.64 ≤ x ≤ 0.76. The longitudinal and the two independent transverse modes that propagate along the [110] crystalline direction were investigated over a range of frequencies from 10 to 150 MHz. Evidence was found for more than one type of motion. The assumption of two simple relaxation processes was sufficient to give a reasonable fit to all of the data. The attempt frequencies for these two processes were found to depend somewhat on H concentration and acoustic mode, but the activation energies did not. The activation energies and approximate attempt frequencies were found to be 0.155 eV and 3 × 10¹² s⁻¹, and 0.254 eV and 10¹⁴ s⁻¹. These values are suggestive, respectively, of tunneling and classical barrier hopping. The relaxation strengths (δC's) derived from the fit *do not* satisfy the Cauchy relation, which means that central forces do not fully describe the H-H interactions. By restricting consideration to nearest- and next-nearest-neighbor H-H interactions, elements of the force-dipole tensor describing H-H interactions are found, including a noncentral force contribution.

INTRODUCTION

Metal-hydrogen systems remain of interest because of their many unusual physical characteristics.¹ Among the striking properties is the very rapid diffusion of H which includes the possibility of tunneling.²⁻⁴ A wide variety of systems have been studied ranging from single crystals to amorphous materials. Even for the simplest systems much is not fully explained. Among the techniques found useful for the study of metal hydrides are ultrasonic attenuation⁵⁻⁷ and internal friction.⁸⁻¹¹ Presented here are the most extensive ultrasonic attenuation measurements to date on a metal hydride, in this case a relatively simple and well-studied one, namely palladium hydride. The temperature and frequency dependence of the attenuation give information about the H hopping rate. Evidence is presented for two types of motion. The magnitude of the attenuation is related to the H-H interaction strength. Results are expressed in terms of a force-dipole tensor.

THEORY

The attenuation is interpreted in terms of relaxation involving the motion of H atoms under the influence of the ultrasonic strain. In the case of a single relaxation time τ the amplitude attenuation coefficient α is given by^{5,12}

$$\alpha = \frac{\omega}{2v} \frac{\delta C}{C} \frac{\omega\tau}{1 + \omega^2\tau^2}, \quad (1)$$

where ω/2π is the ultrasonic frequency, v is the ultrasonic velocity, C is the elastic constant corresponding to the ultrasonic mode propagated, and δC = C^u - C^r where C^r is the relaxed elastic constant¹³ measured at ωτ ≪ 1 and C^u is the unrelaxed elastic constant measured at ωτ ≫ 1. The symmetry of the octahedral site occupied by H in

palladium is such that no relaxation occurs for an isolated H or vacancy. Relaxation occurs due to H-H interactions,⁹ a type of relaxation first proposed by Zener.¹⁴ For the dilute case such that one may consider isolated H-H pairs, calculations¹⁵⁻¹⁸ show that τ is approximately equal to τ_D, the mean time of stay of a particle on an interstitial site. Such calculations have not been carried out for the concentrated case, but a comparison^{13,19} of internal friction data with diffusion measurements on a number of alloys indicates that τ = nτ_D with n of the order 1–10. The data are not usually well described by a single peak as given by Eq. (1), and a distribution of relaxation processes is sometimes used.¹³ A remarkable result of the present study is that the data for three independent ultrasonic modes at various frequencies indicate that a simple Gaussian or Lorentzian distribution of relaxation times does not describe the results. In fact, the data are approximately described as a sum of two peaks of the type given by Eq. (1) with the relative peak heights dependent on acoustic mode.

In addition to information about the hopping rates, the fit of the experimental data to a sum of relaxation processes gives values for the δC's. Theoretical expressions for the δC's for Zener relaxation in concentrated binary alloys have been developed by Le Claire and Lomer,²⁰ and Welch and Le Claire.²¹ The results are described in terms of short-range order parameters α^(l)_k, ordering energies V^(l)_k, and the dependence of these quantities on the strain. Here V^(l)_k is the ordering energy for the site in the kth neighbor shell, along the positive direction l relative to an atom at the origin,

$$V^{(l)}_k = V^{AA(l)}_k + V^{BB(l)}_k - 2V^{AB(l)}_k, \quad (2)$$

where V^{AA(l)}_k refers to the interaction energy between two atoms of type A, one located at the origin and one at (l)_k, with similar definitions for V^{BB(l)}_k and V^{AB(l)}_k. For

the present case it is more convenient to use the concept of the force dipole tensor.²² We find that the Welch-Le Claire theory may be expressed in terms of the force dipole language by defining

$$P_{ij}^{AA(l_k)} = -\frac{dV^{AA(l_k)}}{d\epsilon_{ij}}, \quad (3)$$

where $P_{ij}^{AA(l_k)}$ is an element of the force dipole tensor describing the dependence on the strain ϵ_{ij} of the interaction between a pair of atoms of type A , one located at the origin and the other located at (l_k) . With this change the Welch-Le Claire results may be written as

$$\delta C_{ijij} = \frac{Nm_A m_B}{V} \sum_k \sum_l P_{ij}^{(l_k)} \frac{d\alpha_k^l}{d\epsilon_{ij}}, \quad (4)$$

where N/V is the number of sites per unit volume, m_A and m_B are the atom fractions of A and B atoms, respectively, in the binary alloy, and

$$P_{ij}^{(l_k)} = P_{ij}^{AA(l_k)} + P_{ij}^{BB(l_k)} - 2P_{ij}^{AB(l_k)}. \quad (5)$$

The sum over l for shell k ranges over $z_k/2$ positive directions where z_k is the number of atoms in shell k . We now restrict ourselves to the high temperature limit where the short-range order parameters are small and use the Welch-Le Claire results expressed in the present language,

$$\frac{d\alpha_k^l}{d\epsilon_{ij}} = \frac{m_A m_B}{kT} P_{ij}^{(l_k)}. \quad (6)$$

Equation (4) becomes,

$$\delta C_{ijij} = \frac{Nm_A^2 m_B^2}{VkT} \sum_k \sum_l [P_{ij}^{(l_k)}]^2. \quad (7)$$

We now specialize to the case of H on the palladium fcc sublattice so that $N/V = 4/a_0^3$, where a_0 is the lattice constant, and $m_A = x$ the fraction of the octahedral sites occupied by hydrogen atoms H and $m_B = 1 - x$ the fraction of sites occupied by vacancies V . We limit the sum over k to the first two neighbor shells. Then

$$\delta C_{ijij} = \frac{4x^2(1-x)^2}{a_0^3 kT} \left[\sum_l [P_{ij}^{(l_1)}]^2 + \sum_m [P_{ij}^{(m_2)}]^2 \right], \quad (8)$$

where the sum over l is over half the atoms in the first-neighbor shell (the $z_1/2$ positive directions) and similarly the sum over m is over half the atoms in the second neighbor shell. Formally,

$$P_{ij} = P_{ij}^{HH} + P_{ij}^{VV} - 2P_{ij}^{HV}, \quad (9)$$

but we interpret $P_{ij}^{VV} = P_{ij}^{HV} = 0$ in which case $P_{ij} = P_{ij}^{HH}$ which characterizes the interaction between H atoms.

First-neighbor pairs

The 12 first-neighbor pairs constitute orthorhombic elastic dipoles lying along [110]-type directions. In the principal axis system P will be diagonal and of the form

TABLE I. The principal-axes system for nearest-neighbor H-H dipoles. The first column merely labels the various dipoles l ; the next three columns give the x , y , and z directions of the principal axes in terms of crystalline directions.

l	Principal axes		
1	110	$\bar{1}10$	001
2	$\bar{1}10$	$\bar{1}10$	001
3	101	$\bar{1}01$	0 $\bar{1}0$
4	10 $\bar{1}$	101	0 $\bar{1}0$
5	011	0 $\bar{1}1$	100
6	0 $\bar{1}\bar{1}$	011	100

$$\begin{pmatrix} P_1 & 0 & 0 \\ 0 & P_2 & 0 \\ 0 & 0 & P_3 \end{pmatrix}.$$

We take the six positive directions for the first-neighbor pairs as shown in column 2 of Table I. Table I also gives the principal axis system for these six dipoles. [The six negative directions have been taken care of by a factor of two in the derivation of Eq. (4)].

Second-neighbor pairs

The six second-neighbor pairs constitute tetragonal elastic dipoles lying along [100] type directions. Table II gives the principal axis system and column 2 of that table gives the three positive directions. We let Q denote the dipole due to second-neighbor pairs. In the principal axis system Q will have the form

$$\begin{pmatrix} Q_1 & 0 & 0 \\ 0 & Q_2 & 0 \\ 0 & 0 & Q_2 \end{pmatrix}.$$

Transformation to the measurement frame

We propagate ultrasonic waves along the [110] crystal-line direction and we take as our reference frame (the primed frame) [110], $\bar{1}10$, and [001] for the x' , y' , and z' directions. For δC_{ijij} in the primed frame we need P'_{ij} . Therefore it is necessary to transform the P_{ij} (and the Q_{ij}) to the primed frame. There are six dipoles to be transformed for first neighbor pairs and three for second neighbor pairs as indicated by the principal axes systems of Tables I and II. This transformation can be carried out^{13,23} using the standard transformation for a second-rank tensor,

TABLE II. The principal-axes system for next-nearest-neighbor H-H dipoles. The notation is similar to Table I except that m labels the various dipoles.

m	Principal axes		
1	100	010	001
2	010	$\bar{1}00$	001
3	001	100	010

$$P'_{ij} = \sum_{r=1}^3 \sum_{s=1}^3 a_{ir} a_{js} P_{rs}, \quad (10)$$

where a_{ir} is the direction cosine between the r th axis in the principal axis system and the i th axis in the primed system.

One of the required elastic constants corresponds to elastic waves propagating along [110] and polarized along [001] and is $\delta C'_{1313} = \delta C'_{55} = \delta C'_{44} = \delta C_{44} = \delta C$, where we have first changed to the condensed Voigt notation and then to the conventional notation for one of the shear elastic constants in a cubic crystal. The required elements of the force-dipole tensor are P'_4 (first-neighbor interactions) and Q'_4 (second-neighbor interactions) again in Voigt notation. The P'_4 for each of the six l and the Q'_4 for each of the three m are substituted into Eq. (7) to calculate the contributions to δC .

Another required elastic constant corresponds to elastic waves propagating along [110] and polarized along $[\bar{1}10]$ and is $\delta C'_{1212} = \delta C'_{66} = \delta(C_{11} - C_{12})/2 = \delta C'$. The required elements of the force-dipole moment are P'_6 and Q'_6 .

Finally, longitudinal elastic waves along [110] correspond to $C'_{1111} = C'_{11} = (C_{11} + C_{12} + 2C_{44})/2 = C_L$. The appropriate elements of the force-dipole tensor are P'_1 and Q'_1 . The results are

$$\delta C = \frac{4x^2(1-x)^2}{a_0^3 kT} \left[\frac{1}{2}(P_1 - P_2)^2 \right], \quad (11)$$

$$\delta C' = \frac{4x^2(1-x)^2}{a_0^3 kT} \left[\frac{1}{4}(P_1 + P_2 - 2P_3)^2 + \frac{1}{2}(Q_1 - Q_2)^2 \right], \quad (12)$$

$$\begin{aligned} \delta C_L = \frac{4x^2(1-x)^2}{a_0^3 kT} & \left[\frac{1}{12}(P_1 + P_2 - 2P_3)^2 + \frac{1}{2}(P_1 - P_2)^2 \right. \\ & \left. + \frac{2}{3}(P_1 + P_2 + P_3)^2 + \frac{1}{6}(Q_1 - Q_2)^2 \right. \\ & \left. + \frac{1}{3}(Q_1 + 2Q_2)^2 \right]. \quad (13) \end{aligned}$$

Equation (11) shows that second-neighbor interactions do not affect δC for the symmetry considered here.

It is interesting to note that if we take $P_2 = P_3 = Q_2 = 0$, then Eqs. (11)–(13) give

$$\delta C_L = 2\delta C + \delta C'. \quad (14)$$

Equation (14) may also be written as $\delta C_{12} = \delta C_{44}$ a Cauchy relation⁵ for the δC 's. The Cauchy relation for the ordinary elastic constants is well known to follow from the assumption of central forces and inversion symmetry. Taking only one element for the force-dipole tensor is equivalent to the assumption of central forces. (It is sometimes stated, incorrectly, that the central force assumption is equivalent to taking only one element of the λ tensor.)

EXPERIMENTAL DETAILS

The preparation of the samples has been described previously.²⁴ Briefly, a single crystal of palladium, approximately 1 cm in diameter and 0.75 cm long, was prepared

with flat and parallel faces for propagation of ultrasonic waves along the [110] direction. The sample was annealed in vacuum at 800°C for one hour and then charged with hydrogen in a pressure cell and furnace. Temperature and pressure were controlled so as to avoid both the mixed phase region, and hydrogen concentration gradients greater than 1%. The sample was first charged to a hydrogen concentration of $x = 0.72$. Hydrogen was allowed to evolve for several days at room temperature and atmospheric pressure until the concentration reached 0.67 at which point the measurements were made. To prevent further escape of hydrogen, the sample was stored in liquid nitrogen when measurements were not being made. After the $x = 0.67$ measurements were completed, the hydrogen was removed, again by avoiding both the mixed-phase region and large concentration gradients. Careful records were kept of the weight of the sample using a microbalance with a resolution of 0.1 mg. To a sensitivity of 20 ppm the weight of the sample before charging and after discharging the hydrogen was the same. The same sample was then charged to a concentration of 0.76 using the same process. The $x = 0.76$ sample was first treated with a potassium-iodide solution to slow the escape of hydrogen and then plated with a copper film which reduced the escape rate to a negligible level. The sample was always stored in liquid nitrogen when not used in the experiments. After the 0.76 measurements were finished, the copper film was removed. The sample was kept at 47°C for 35 days after which time the hydrogen concentration was 0.72. The sample was replated with copper and ultrasonic measurements were performed. The copper film was removed and the sample lightly polished with 0.05 μm powder to allow the hydrogen to evolve more freely. After the concentration reached 0.64 another series of ultrasonic measurements were made.

Ultrasonic waves were propagated along the [110] direction. Longitudinal waves, transverse waves polarized along [001], and transverse waves polarized along $[\bar{1}10]$ were investigated. These correspond to the elastic constants

$$\begin{aligned} C_L &= \frac{1}{2}(C_{11} + C_{12} + 2C_{44}), \\ C &= C_{44}, \\ C' &= \frac{1}{2}(C_{11} - C_{12}). \end{aligned} \quad (15)$$

The standard ultrasonic pulse-echo method was used to measure the attenuation. The heights of two echoes were measured to minimize effects of losses in the bonding material used to attach the quartz piezoelectric transducers to the sample.

RESULTS AND DISCUSSION

Figures 1–3 give attenuation data for the three independent acoustic modes as a function of H concentration for a frequency of approximately 10 MHz. The peak shifts to higher temperature as the H concentration is increased for all three modes. It is also seen that at the lower concentrations the peak occurs at a lower temperature for the C mode than for the other two modes. This

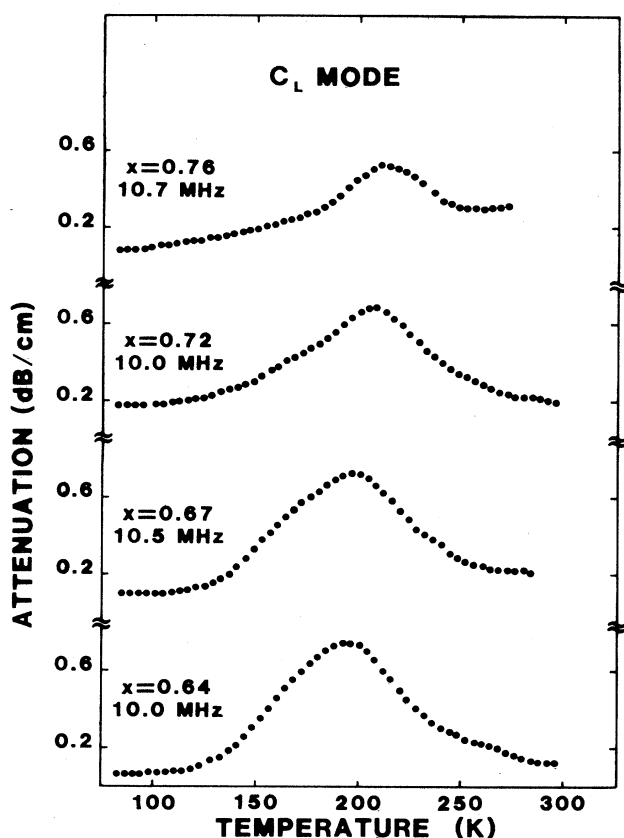


FIG. 1. Ultrasonic attenuation vs temperature for longitudinal waves propagating along the [110] direction (C_L mode) in single-crystal α' phase PdH_x for various x values. The ultrasonic frequencies are listed in the figure.

effect has been seen previously.⁵ (The 10.7 MHz data for longitudinal waves in the $x=0.76$ sample show a strong temperature dependent background. Such a background was not observed for any other case, e.g., higher-frequency longitudinal waves in the $x=0.76$ sample did not show this effect. A special relationship between the thickness of the copper film and the ultrasonic wavelength may have led to high losses in the copper film or ultrasonic bond for this particular data set. These data were not used in the following analysis.)

At each of the four concentrations and for each of the three modes, measurements were performed as a function of frequency. An average relaxation time may be found by taking $\omega\tau=1$ at the attenuation maximum. The frequency dependent data may be displayed in an Arrhenius plot to determine an activation energy and attempt frequency associated with the peak position. The results for longitudinal waves are given in Fig. 4 for each concentration. The thermally activated relaxation time determined in this way may then be used in Eq. (1) to calculate the attenuation over the entire temperature range. From such a calculation it is clear that a single Debye peak is too narrow to fit the experimental results.

The usual approach to fit such data is to use a distribu-

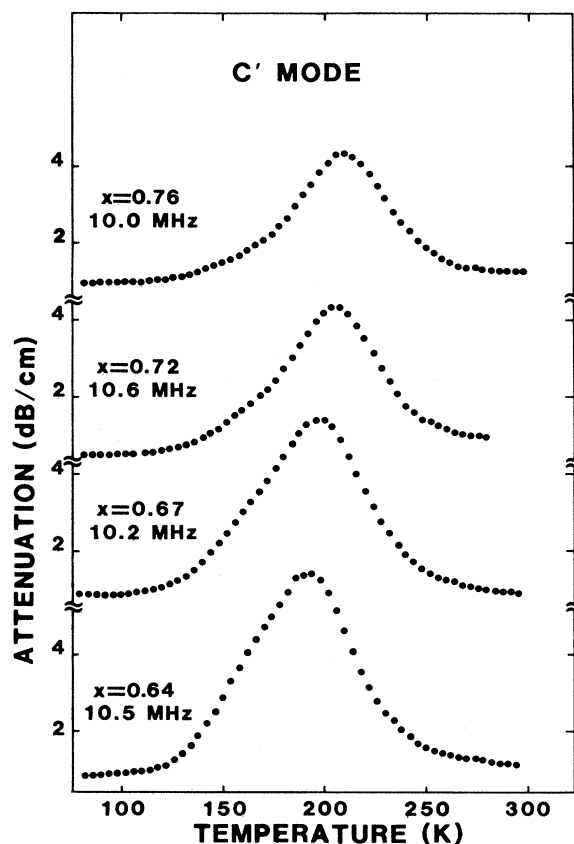


FIG. 2. Same as Fig. 1, except transverse waves propagating along [110] polarized along $[\bar{1}10]$ (C' mode).

tion of relaxation times. Indeed, we found that such an approach with an asymmetric Gaussian distribution of activation energies,²⁵ gave a reasonable fit to the C_L mode and C' mode data for the various frequencies and concentrations studied. In addition, an approach using a symmetric Gaussian distribution of activation energies and the Zener relation²⁶ between activation energy and attempt frequency was also capable of fitting the C_L and C' mode data. However, the results for the C mode, especially at the higher concentrations, are very poorly described by such approaches. The data suggest a bimodal distribution.

We take the simplest approach and attempt to fit all the data as a sum of two simple Debye peaks. Using $C=\rho v^2$ where ρ is the sample density, and Eq. (1) we take

$$\alpha = \frac{\omega}{2\rho v^3} \sum_{i=1}^2 \left[\delta C_i \frac{\omega\tau_i}{1+\omega^2\tau_i^2} \right], \quad (16)$$

where

$$\tau_i = \tau_{0i} \exp(E_{0i}/kT),$$

and we assume

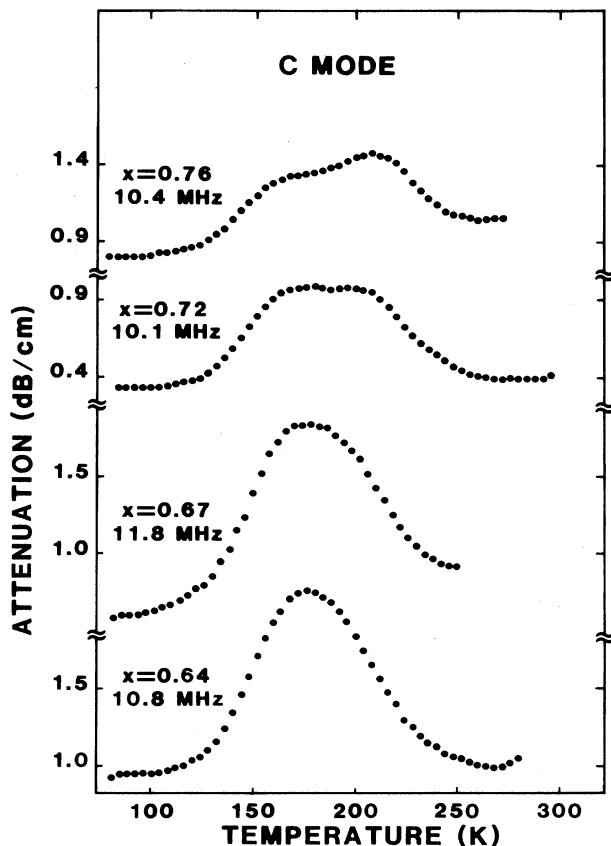


FIG. 3. Same as Fig. 1, except transverse waves propagating along [110] polarized along [001] (C mode).

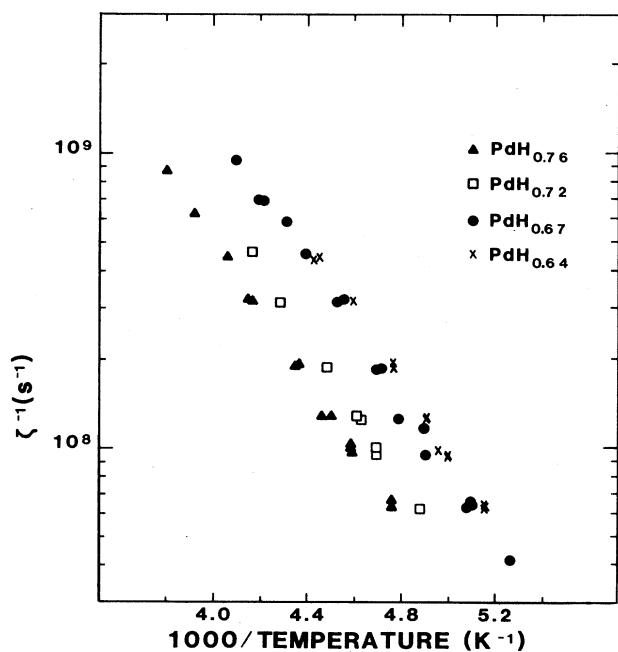


FIG. 4. Average relaxation times (determined by setting $\omega\tau=1$ at the attenuation maxima) vs inverse temperature. Longitudinal waves were propagated along the [110] direction.

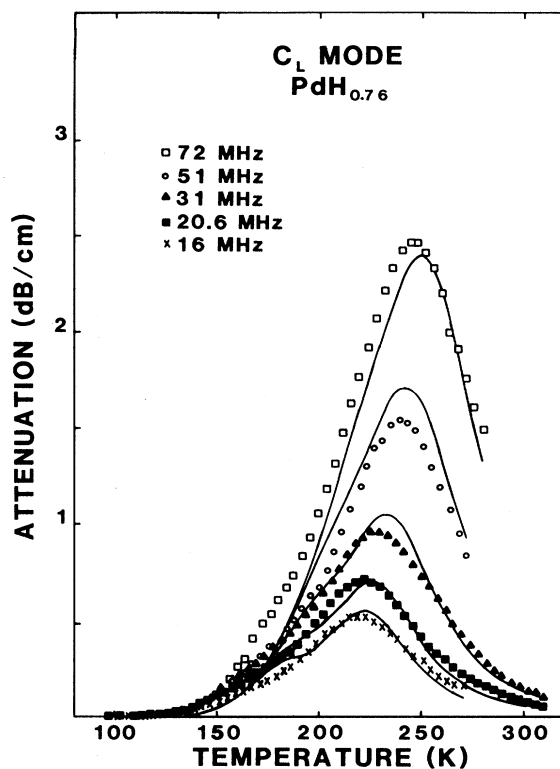
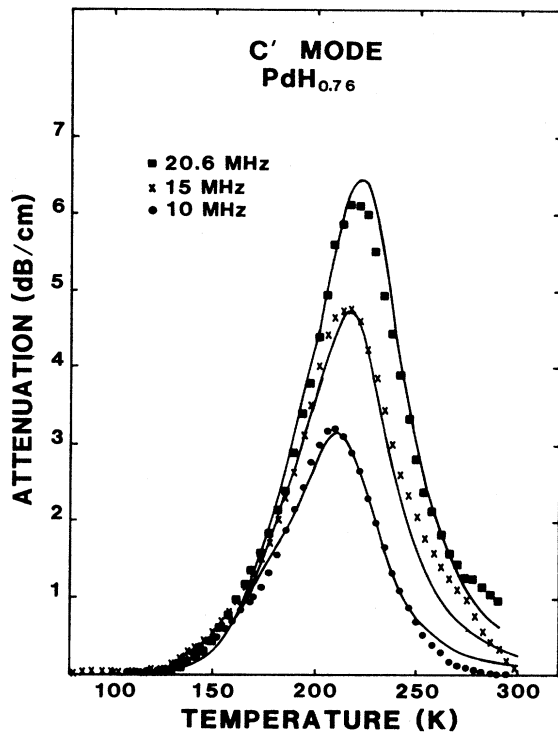
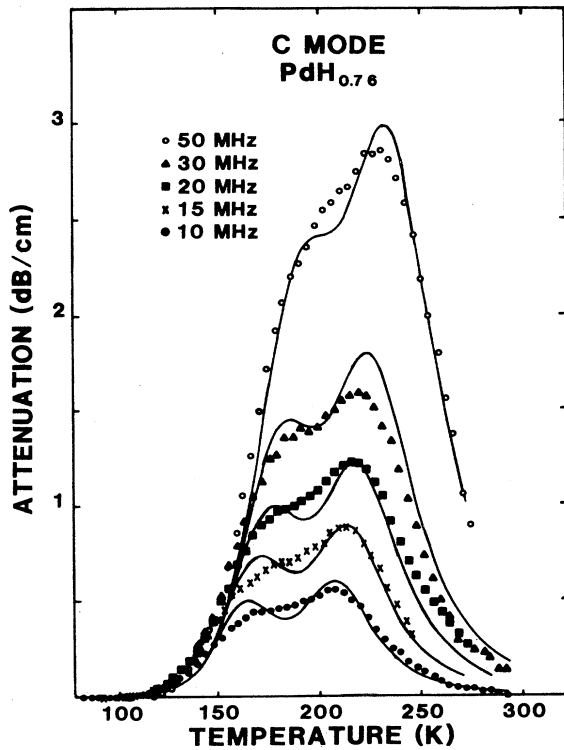


FIG. 5. Ultrasonic attenuation at various frequencies for longitudinal waves along [110] in $\text{PdH}_{0.76}$. The points represent the data while the solid lines represent the sum of two Debye peaks.

$$\delta C_i = \frac{A_i}{T}$$

The fitting parameters are then E_{0i} , τ_{0i} , and A_i , giving a total of six parameters to fit the frequency and temperature dependence of each mode at each concentration. We require, however, E_{0i} to be independent of acoustic mode. In addition, we do not expect τ_{0i} to depend strongly on acoustic mode. A strong mode dependence would be difficult to understand. These parameters may, of course, be concentration dependent. For a given concentration and acoustic mode we fit all frequencies simultaneously over the entire temperature range. The results for all the longitudinal data at $x=0.76$ are given in Fig. 5. Figures 6 and 7 give results for the C' and C modes, respectively.

The overall features are reasonably well described by this fitting procedure. These features include the shift in position with concentration shown in Figs. 1–3, the fact that at lower concentrations the C mode attenuation reaches a maximum at a lower temperature than the other modes, and the strong mode and concentration dependence of the peak shapes. The theoretical peaks obviously show more structure than the data. Although we do not show the results here, the addition of a small distribution of activation energies to each subpeak largely eliminates this structure.²⁷ Nevertheless, the calculated peaks

FIG. 6. Same as Fig. 8 except for the C' mode.FIG. 7. Same as Fig. 8 except for the C mode.

still show differences from the data and the description purely in terms of two subpeaks is probably an oversimplification. It is remarkable, however, to get an approximate fit to such a vast range of data (frequency, concentration, temperature, and mode dependences) with such a simple approach.

We turn now to a discussion of the fitting parameters. We find that the activation energies are essentially the same for all the concentrations: we find $E_1=0.155$ eV and $E_2=0.254$ eV for the low-temperature and high-temperature subpeaks, respectively. Other experiments²⁸ have shown evidence of two different activation energies approximately equal to those we find.

The other parameters are displayed in Fig. 8. It is encouraging that the attempt frequency does not depend strongly on the acoustic mode. The consistency of the results is remarkable. With only two exceptions, the attempt frequency for the C' mode lies between those for the other two modes. It is found, however, that the attempt frequencies associated with the two subpeaks differ by more than an order of magnitude. Also shown in Fig. 8 is the classical single *particle* attempt frequency calculated from $\tau_0^{-1}=Z(1-x)\nu_0^0$, where Z is the number of nearest neighbor octahedral sites (12 in the present case),

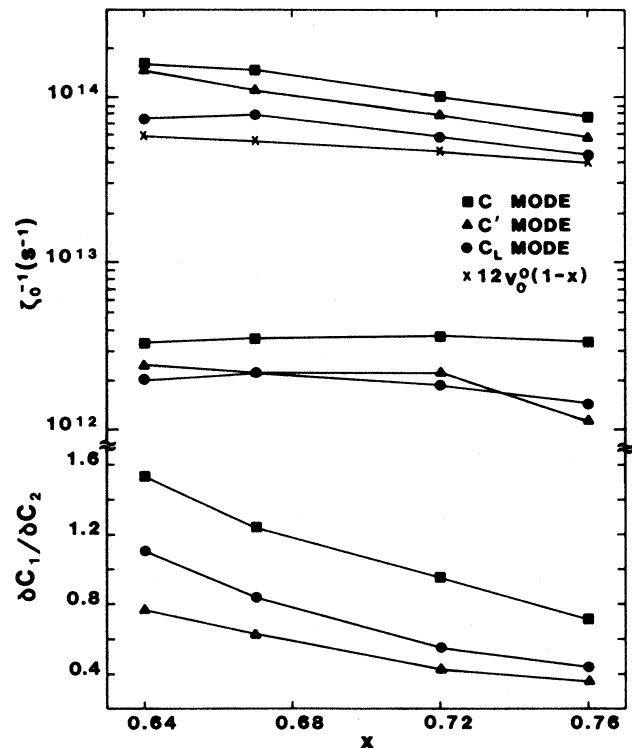


FIG. 8. Fitting parameters vs H concentration. The upper part shows the two attempt frequencies for each mode. The activation energies associated with the low and high attempt frequencies are 0.155 and 0.254 eV, respectively. The classical single-particle attempt frequency is also shown. The lower part shows the ratios of relaxation strengths for the two Debye peaks for the three acoustic modes. δC_1 and δC_2 are associated with the low activation energy (low attempt frequency) and high activation energy (high attempt frequency), respectively.

and ν_0^0 is the vibrational frequency of H in its potential well calculated from neutron scattering to be $1.4 \times 10^{13} \text{ sec}^{-1}$. It is remarkable that the classical expression agrees within a factor of 2 with the experimental results for all three acoustic modes for the high-temperature component. Although the agreement may be fortuitous, the result at least suggests that the high-temperature component corresponds to classical barrier hopping.

As mentioned above, the low-temperature subpeak has a much lower attempt frequency than the high-temperature subpeak. It has been shown that hopping may occur by a transition to an excited state in the well followed by tunneling from the excited state.^{2,3} The effective attempt frequency for this process may be much lower than that characteristic of classical hopping. Therefore, it may well be that the low-temperature subpeak corresponds to tunneling. In this connection it is interesting to note that tunneling may be especially sensitive to strain in the material.³ The samples used in the present study were large single crystals carefully prepared to avoid internal strains. These samples have a relatively high density²⁴ which is associated with low strains.

Each subpeak for each mode is characterized by a δC . The ratios of the low temperature subpeak to the high-temperature subpeak δC 's are given in the bottom part of Fig. 8. It is seen that, relative to the high-temperature peak, the low-temperature peak decreases with increasing concentration. (It is this decrease which causes the overall peak to shift to higher temperature as the H concentration is increased.) Interpreted as tunneling, this decrease means, of course, that tunneling is more likely at lower hydrogen concentrations. This trend is opposite to what would be expected if tunneling only occurs between sites for which the H atom has the same number of nearest-neighbor sites occupied by H before and after the transition (assuming random-site occupancy).

Figure 8 also shows that the ratio has a definite dependence on ultrasonic mode. We now make some speculative remarks about that dependence. We assume that the relaxation strength may be described in terms of first- and second-neighbor interactions. (For the concentrations considered here it is convenient to think of vacancy pairs. Rather than H-H interactions we can think of effective $V-V$ interactions.) In a central force description, δC is not at all affected by second neighbor interactions, $\delta C'$ is strongly affected by these interactions, and δC_L is affected, but not nearly so strongly as $\delta C'$. This result is well known for the ordinary elastic constants,²⁹ has been derived previously⁵ for the δC 's, and follows from Eqs. (11)–(13) in the central-force approximation. Figure 8 shows that the low temperature component is inversely correlated with second-neighbor interactions. For relaxation strengths dependent only on first-neighbor interactions the low-temperature component is relatively prominent. For relaxation strengths dependent relatively more strongly on second-neighbor interactions, the low-temperature peak is much weaker relative to the high-temperature component. If the low-temperature peak is indeed due to tunneling then this correlation with second-neighbor interactions must be related to the microscopic environment in which tunneling occurs.

TABLE III. The relaxation strengths, δC_L , δC , and $\delta C'$ for different H concentrations x in units of 10^8 N/m^2 .

x	δC_L	δC	$\delta C'$
0.64	8.17	1.78	2.33
0.67	6.95	1.58	1.99
0.72	5.04	1.27	1.54
0.76	3.94	1.01	1.32

By fitting the entire attenuation versus temperature curve for various frequencies, we derive values for the δC 's. The accuracy of these values depends on the quality of the fit to the experimental curve, and does not depend on the detailed physical interpretation of the origin of the two subpeaks. Results are shown in Table III for a temperature of 200 K.

If central forces describe the H-H interactions, then the δC 's should satisfy a Cauchy relation, just as for the ordinary elastic constants. The usual statement is that $C_{12} = C_{44}$ for central forces. We can extract δC_{12} from the measured δC_L , $\delta C'$, and δC_{44} . Figure 9 shows the ratio $\delta C_{44}/\delta C_{12}$ as a function of concentration. The results are similar to the ratio C_{44}/C_{12} for the ordinary elastic constants in both pure Pd and PdH_x which is³⁰ approximately 0.4. Although not described in the present paper, we have also used a *three-peak* approach to fit the results.²⁷ The δC 's derived from this approach are about 20% higher than those resulting from the two-peak approach, but the relative values are essentially the same for the two approaches. The results from the three-peak fit are also shown in Fig. 9. Central forces do not give a

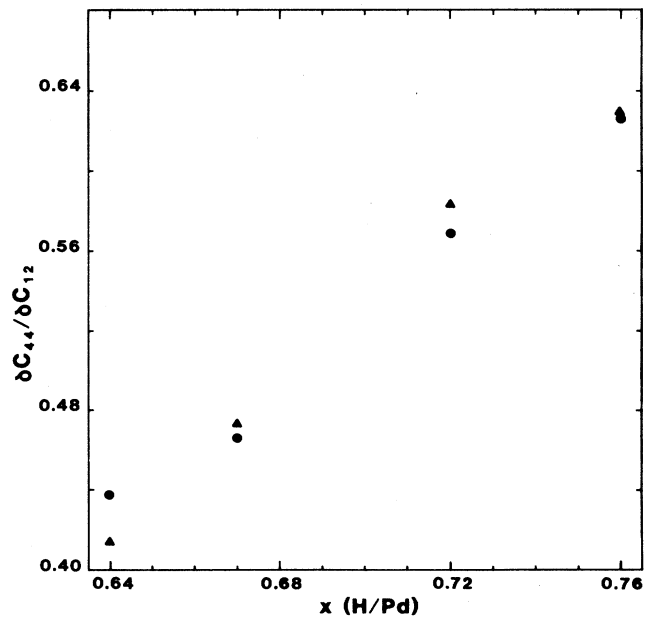


FIG. 9. The Cauchy ratio $\delta C_{44}/\delta C_{12}$ vs H concentration. The dots represent results derived from the two-peak fit to the data described in the text. The triangles result from a three-peak fit to the data.

TABLE IV. Force-dipole elements for various H concentrations x . P denotes nearest-neighbor interactions and Q denotes next-nearest-neighbor interactions.

x	$ P_1 - P_2 $ (eV)	$ P_1 + 2P_2 $ (eV)	$ Q_1 $ (eV)
0.64	0.109	0.152	0.098
0.67	0.107	0.146	0.093
0.72	0.105	0.132	0.089
0.76	0.104	0.125	0.094

good description of the results, although the ratio tends toward unity as the H concentration is increased. An earlier measurement⁵ at a single concentration and for a single-frequency indicated that the δC 's did obey a Cauchy relation. The present results are felt to be much more reliable.

Equations (11)–(13) give the δC 's in terms of the elements of the force-dipole tensor describing H-H interactions for first and second neighbor pairs. It is seen that five elements of the force dipole element are involved while there are only three independent δC 's. Some simplifying approximations are necessary. Neutron scattering measurements³¹ shows that second neighbor interactions are important, thus we want to keep a contribution from this source. We simplify the noncentral force contributions by taking $P_2 = P_3$, $Q_2 = 0$.

With this simplification the force-dipole elements given in Table IV are derived from the data in Table III using Eqs. (11)–(13). From the experimental results we can only determine absolute values for the quantities listed in Table IV. If $(P_1 - P_2)$ and $(P_1 + 2P_2)$ have the same sign, then it turns out that P_1 and P_2 also have the same sign for all cases and $|P_2| \ll |P_1|$. With opposite signs $|P_2|$ is considerably greater than $|P_1|$. It seems likely that the same sign situation applies. Table V gives results under the assumption of same signs. It is seen that the Cauchy ratio is a sensitive test for central forces since a small P_2 contribution causes the Cauchy ratio to deviate markedly from unity. The weak concentration dependence of $|P_1|$ and $|Q_1|$ is in accord with neutron scattering measurements³² of the dispersion curves in palladium *deuteride* which show very little concentration dependence. McKergow *et al.*³² have used a spherically symmetric potential to fit the dispersion curve measurements on PdD_{0.8}. Their potential gives $P_1 = 0.41$ eV, $P_2 = 0$, and $Q_1 = 0.16$ eV. These values are somewhat higher than our values as shown in Tables IV and V. It was pointed out,³² however, that substantially different sets of force constants have been used to describe the dispersion curve measurements.

We have also calculated the force-dipole elements from the three-peak fit to the data. The various elements are about 10% higher than those found from the two-peak

TABLE V. Nearest-neighbor force-dipole elements with the assumption that $(P_1 - P_2)$ and $(P_1 + 2P_2)$ have the same sign.

x	$ P_1 $ (eV)	$ P_2 $ (eV)
0.64	0.123	0.014
0.67	0.120	0.013
0.72	0.115	0.009
0.76	0.111	0.007

approach, but the results for the concentration dependence and the relative magnitudes of the various elements are essentially the same as for the two-peak fit. This is in accordance with the earlier statement that the results for the δC 's should depend on the quality of the fit to the experimental data, and not on the detailed interpretation of the relaxation processes involved.

CONCLUSIONS

Extensive ultrasonic measurements on single-crystal PdH_x show evidence for two types of motion. A simple model incorporating two Debye peaks allows us to fit the data over a wide range of temperature, H concentration, and ultrasonic frequency for all three independent ultrasonic modes. The activation energies and attempt frequencies derived from the fit are suggestive of tunneling and classical barrier hopping. The relative contribution of the peak associated with tunneling decreases as the H concentration increased. Also, this peak is less pronounced for those ultrasonic modes sensitive to second neighbor interactions. It is suggested that the large, low-strain, single crystals used in the study may be especially favorable for tunneling. The violation of the Cauchy relation for the δC 's indicates that central forces are an inadequate description of H-H interactions. This conclusion does not depend on any restrictive assumption about the range of the interaction. By restricting consideration to first and second neighbor H-H interactions, elements of the force-dipole tensor describing H-H interactions are found, including a noncentral force contribution. With a simple assumption about relative signs, it is found that the noncentral force contribution is only about 10% of the central force contribution, and decreases with increasing H concentration. The central force contributions are only weakly concentration dependent.

ACKNOWLEDGMENTS

This work was supported by the National Science Foundation under Grant No. DMR-80-12689.

*Present address: Rosemount Corporation, Corporate Technology, Eden Prairie, MN 55344.

¹See E. Wicke and H. Brodowski, in *Hydrogen in Metals II*, Vol. 29 of *Springer Topics in Applied Physics*, edited by G. Alefeld and J. Volkl (Springer-Verlag, Berlin, 1978), p. 73.

²R. R. Arons, in *Proceedings of the International Conference on Vacancies and Interstitials in Metals*, Julich, 1968, edited by A. Seeger (North Holland, Amsterdam, 1970).

³I. Svare, *Physica B+C* **141B**, 271 (1986).

⁴K. W. Kehr, in *Hydrogen in Metals I*, Vol. 29 of *Springer To-*

- pics in Applied Physics*, edited by G. Alefeld and J. Volkl (Springer-Verlag, Berlin), 1978, p. 197.
- ⁵R. G. Leisure, T. Kanashiro, P. C. Reidi, and D. K. Hsu, *Phys. Rev. B* **27**, 4827 (1983).
- ⁶R. G. Leisure, T. Kanashiro, P. C. Reidi, and D. K. Hsu, *J. Phys. F* **13**, 2025 (1983).
- ⁷R. G. Leisure, L. A. Nygren, and D. K. Hsu, *Phys. Rev. B* **33**, 8325 (1986).
- ⁸R. R. Arons, Y. Tamminga, and G. de Vries, *Phys. Status Solidi* **40**, 107 (1970).
- ⁹G. J. Zimmermann, *J. Less-Common Met.* **49**, 49 (1976).
- ¹⁰F. M. Mazzolai, M. Nuovo, and F. A. Lewis, *Nuovo Cimento* **33B**, 242 (1976).
- ¹¹F. M. Mazzolai, P. G. Bordoni, and F. A. Lewis, *J. Phys. F* **11**, 337 (1981).
- ¹²A. B. Bhatia, *Ultrasonic Absorption* (Clarendon, Oxford, 1967).
- ¹³A. S. Nowich and B. S. Berry, *Anelastic Relaxation in Crystal-line Solids* (Academic, New York, 1972).
- ¹⁴C. Zener, *Phys. Rev.* **71**, 34 (1947).
- ¹⁵A. D. Franklin, *J. Res. NBS A* **67**, 291 (1963).
- ¹⁶R. Chang, *J. Phys. Chem. Solids* **25**, 1081 (1964).
- ¹⁷R. W. Dreyfus and R. B. Laibowitz, *Phys. Rev.* **135**, A1413 (1964).
- ¹⁸Y. Haven, *Phys. Status Solidi* **26**, 653 (1968).
- ¹⁹C. Wert, in *Physical Acoustics*, edited by W. P. Mason (Academic, New York, 1966), Vol. 8.
- ²⁰A. D. Le Claire and W. M. Lomer, *Acta Metall.* **2**, 731 (1954).
- ²¹D. O. Welch and A. D. Le Claire, *Philos. Mag.* **16**, 981 (1967).
- ²²R. Siems, *Phys. Status Solidi* **30**, 645 (1968).
- ²³J. F. Nye, *Physical Properties of Crystals* (Clarendon, Oxford, 1957).
- ²⁴L. A. Nygren, Y. Cho, D. K. Hsu, and R. G. Leisure, *J. Phys. F* **18**, 1127 (1988).
- ²⁵B. S. Berry and W. C. Pritchett, *Phys. Rev. B* **24**, 2299 (1981).
- ²⁶C. Zener, *J. Appl. Phys.* **22**, 372 (1951).
- ²⁷L. A. Nygren, Ph.D. thesis, Colorado State University, 1987 (unpublished).
- ²⁸F. M. Mazzolai and H. Züchner, *Z. Phys. Chem. Neue Folge* **124**, 59 (1981).
- ²⁹M. J. P. Musgrave, *Crystal Acoustics* (Holden-Day, San Francisco, 1970).
- ³⁰L. A. Nygren and R. G. Leisure, *Phys. Rev. B* **37**, 6482 (1988).
- ³¹J. M. Rush, J. J. Rush, H. G. Smith, M. Mostoller, and H. E. Flotow, *Phys. Rev. Lett.* **33**, 1297 (1974).
- ³²M. W. McKergow, P. W. Gilbred, D. J. Picton, D. K. Ross, P. Fratzl, O. Blashko, I. S. Anderson, and M. Hagen, *Z. Phys. Chem. Neue Folge* **146**, 159 (1985).
- ³³A. Rahman, K. Skold, C. Pellizari, S. K. Sinha, and H. Flotow, *Phys. Rev. B* **14**, 3630 (1976).